ELEMENTA
Science of the Anthropocene

Ebling, AM and Landing, WM 2017 Trace elements in the sea surface microlayer: rapid responses to changes in aerosol deposition. *Elem Sci Anth,* 5: 42, DOI: https://doi.org/10.1525/elementa.237

RESEARCH ARTICLE

Trace elements in the sea surface microlayer: rapid responses to changes in aerosol deposition

Alina M. Ebling*,† and William M. Landing†

Natural and anthropogenic aerosols are a significant source of trace elements to oligotrophic ocean surface waters, where they provide episodic pulses of limiting micronutrients for the microbial community. However, little is known about the fate of trace elements at the air-sea interface, i.e. the sea surface microlayer. In this study, samples of aerosols, sea surface microlayer, and underlying water column were collected in the Florida Keys during a dusty season (July 2014) and non-dusty season (May 2015) and analyzed for the dissolved and particulate elements Al, Fe, Ni, Cu, Zn, and Pb. Microlayer samples were collected using a cylinder of ultra-pure SiO_2 (quartz glass), a novel adaptation of the glass plate technique. A significant dust deposition event occurred during the 2014 sampling period which resulted in elevated concentrations of trace elements in the microlayer. Residence times in the microlayer from this event ranged from 12 to 94 minutes for dissolved trace elements and from 1.3 to 3.4 minutes for particulate trace elements. These residence times are potentially long enough for the atmospherically derived trace elements to undergo chemical and biological alterations within the microlayer. Characterizing the trace element distributions within the three regimes is an important step towards our overall goals of understanding the rates and mechanisms of the solubilization of trace elements following aeolian dust deposition and how this might affect microorganisms in surface waters.

Keywords: sea surface microlayer; trace elements; aerosols; residence times; dust deposition

Introduction

Atmospheric deposition is an important source of bioactive trace elements to the surface ocean and can play a large role in marine primary productivity (Boyd et al., 2010; Baker et al., 2016). In particular, the deposition of mineral dust to the open ocean has received increasing attention (Duce and Tindale, 1991; Baker et al., 2016), as it is a major source of Fe, a known limiting micronutrient (e.g., Martin and Gordon, 1988). Other biologically relevant trace elements such as Ni, Cu, and Zn derived from atmospheric deposition play important roles in enzymatic processes and may influence phytoplankton productivity (e.g., Dupont et al., 2010; Mackey et al., 2015 and references therein). There have been many studies on the cycling of atmospherically derived Fe and other trace elements in the surface ocean (e.g., Prospero, 1999; Baker and Croot, 2010 and references therein; Buck et al., 2010); however, little research has focused on the air-sea interface where trace elements initially enter the water column.

The sea surface microlayer is the thin, organic-rich layer at the air-sea interface covering approximately 71% of the Earth's surface (Franklin et al., 2005; Cunliffe et al., 2009). Generally defined as 10 to 1,000 μm in thickness (Cunliffe et al., 2013), the microlayer is enriched in organic compounds that create a semi-rigid film-like layer over the surface ocean. Due to this organic enrichment, the microlayer has physicochemical and biological properties that are different from the underlying water column (Hardy, 1982; Liss and Duce, 2005; Cunliffe et al., 2013), making it a unique environment.

The microlayer is the physical link between the sea surface and lower atmosphere and is therefore linked to the biogeochemical cycling of trace elements and other compounds in the marine environment (Liss and Duce, 2005). The presence of surface-active organic compounds within the microlayer can alter the chemical composition of the aerosols. Baker and Croot (2010) emphasize that the presence of ligands and surfactants within the microlayer would enhance the dissolution of atmospherically derived Fe. There are two dominant fluxes of trace elements to the microlayer: rising bubbles and atmospheric deposition. Previous research showed that the microlayer was elevated in particulate trace elements compared to the water column (e.g., Barker and Zeitlin, 1972; Duce et al., 1972; Brügmann et al., 1992; Grotti et al., 2001); however, these observations alone are not enough to deconvolute and

* Department of Earth, Ocean and Atmospheric Science, Florida State University, Tallahassee, Florida, US

† Department of Marine Chemistry and Geochemistry, Woods Hole Oceanographic Institution, Woods Hole, Massachusetts, US

Corresponding author: Alina M. Ebling (aebling@whoi.edu)

quantify the sources of trace elements to the microlayer. The solubility of Fe in seawater (pH 8.1) can be as low as 0.01 nM (Liu and Millero, 2002). However, the presence of organic ligands can increase the solubility of Fe greater than ten-fold (Gledhill and Buck, 2012), making it more bioavailable. The enhanced solubilization of aerosol Fe as well as other trace elements could have profound impacts on primary productivity, yet there is a lack of data specifically addressing the solubilization of trace elements by organic compounds in the microlayer or the potential biological responses resulting from this process.

The goal of this study was to determine the fate of atmospheric aerosols in the microlayer. Specifically, we measured the concentrations of dissolved and particulate Al, Fe, Ni, Cu, Zn, and Pb in the microlayer, water column, and aerosols in the Florida Keys during the spring and summer months. These elements, except Al and Pb, are bioactive trace elements important in primary productivity (Morel and Price, 2003). Al and Pb are used as tracers of aerosols: Al for lithogenic sources and Pb for anthropogenic sources.

Methods

Study sites

Sampling took place during two field campaigns in the Florida Keys (**Figure 1**), one during a "dusty" season (July 2014) and one during a "non-dusty" season (May 2015). For a typical July "dusty" season, the dust flux is approximately 17 mg m^{-2} d^{-1} in this region (Prospero and Mayol-Bracero, 2013). Sea surface microlayer and underlying water column sampling took place July 25 through 27, 2014, approximately 500 m offshore of the Keys Marine Laboratory, Layton, FL, USA (lat: 24.825832, long: –80.814262) in the Florida Bay (FB) and July 28, 2014, approximately 700 m offshore of Curry Hammock State Park, Marathon, FL, USA (lat: 24.740892, long: –80.981041) in the coastal Atlantic Ocean (AO). Aerosol samples were collected July 23 through 28, 2014, in Curry Hammock State Park. For a typical May "non-dusty" season, the dust flux is approximately 4.3 mg m^{-2} d^{-1} in this region (Prospero and Mayol-Bracero, 2013). Microlayer and water column sampling took place May 5 through 9, 2015, approximately 1,000 m offshore of the MOTE Tropical Research Laboratory, Summerland Key, FL, USA (lat: 24.740892, long: –81.981041) in the Summerland Key Bay (SB), and May 6 and 9, 2015, approximately 14 km offshore at the Looe Key National Marine Sanctuary (lat: 24.550933, long: –81.417201; LK). Aerosol samples were collected May 4 through 10, 2015, at MOTE.

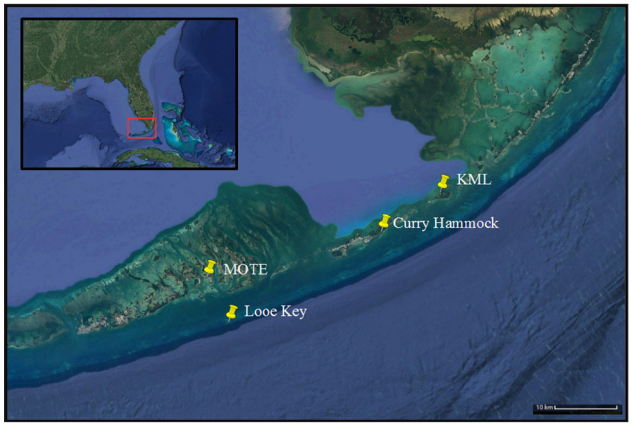

Figure 1: Sampling locations. Locations of the sampling sites during the field campaigns in 2014 from the Keys Marine Laboratory (KML, in Florida Bay) and Curry Hammock State Park (in the coastal Atlantic Ocean), and in 2015 from MOTE Tropical Research Laboratory and Looe Key National Marine Sanctuary. Scale bar is 10 km. DOI: https://doi.org/10.1525/elementa.237.f1

Sea surface microlayer and underlying water column sample collection and analysis

Sea surface microlayer samples were collected from a plastic kayak using a hollow quartz tube sampling device described in Ebling and Landing (2015). Briefly, the quartz tube was dipped vertically into the water column until most of the surface area below the handle was submerged. It was then slowly pulled vertically out of the water (5–10 cm s^{-1}) and held over a funnel attached to a receiving bottle where the microlayer sample dripped off the quartz tube. This process was repeated until 125 to 550 mL of sample was collected. Corresponding underlying water column samples (30 cm depth) were also collected from the kayak wherein a closed bottle was submerged under water, opened, and closed again underwater to prevent mixing with the microlayer. Shoulder-length polyethylene gloves were worn to minimize trace element contamination. Immediately after sample collection, the microlayer and water column samples were filtered using 47 mm 0.2 µm polycarbonate track-etched (PCTE) membrane filters by vacuum filtration. The seawater samples were acidified with 6 M quartz distilled HCL (q-HCl) to a final concentration of 0.024 M q-HCl and the filters were frozen until analysis.

The microlayer and water column samples were analyzed for dissolved, reactive particulate, and refractory particulate trace element concentrations. Dissolved trace elements were pre-concentrated and extracted from the high salt content of seawater by a cation exchange column method described in Milne et al. (2010). Reactive particulate trace elements were leached from the filters using a 4.4 M acetic acid (q-HAc) with 0.02 M hydroxylamine hydrochloride (HH) solution as described in Berger et al. (2008). Refractory particulate trace elements were digested using microwave digestion with concentrated (15.8 M) q-HNO_3 and concentrated (28 M) HF (*Optima*) to dissolve the residual particulate matter (Ebling and Landing, 2015). All samples were analyzed using a Thermo-Scientific Element 2 (E2) high resolution inductively-coupled plasma mass spectrometer (HR-ICP-MS). Reactive and refractory particulate concentrations were summed to calculate the total particulate trace element concentrations in the microlayer and water column. For the dissolved trace elements, analytical precision was determined through replicate analysis of deep (1000 m, SAFe-D2) seawater samples from the SAFe inter-comparison project (Johnson et al., 2007). For the reactive particulate trace elements, analytical precision was determined through replicate analysis of a multi-element check standard on the E2 HR-ICP-MS as

there is currently no standard reference material for reactive particulate suspended matter (Ebling and Landing, 2015). Certain refractory trace elements such as Ti and Zr have very low solubility in the reactive leach solution. Low concentrations of such elements in the leach solution helps to demonstrate that small refractory particles were not carried over into the samples, and were therefore monitored for all particulate samples in this study. For the refractory particulate trace elements, analytical precision was determined through replicate analysis of the sediment standard reference material NIST-2704 (Buffalo River Sediment).

Aerosol sample collection and analysis

Aerosol samples, integrated over 24 hours, were collected using a high-volume aerosol sampler (model 5170-VBL, Tisch Environmental) which pulls air at approximately 1.2 m^3 min^{-1} through 12 replicate acid-washed 47 mm nitrocellulose filter disks (Whatman 41). Filters were frozen until analysis.

Instantaneous aerosol leaches (a.k.a. UHP-soluble) were conducted using the method described in Buck et al. (2010); very rapid flow-through leaching (10–20 seconds) using 100 mL of ultra-high purity (UHP) deionized water (>18 MΩ*cm; pH = 6.0). Total aerosol digestions were conducted using a microwave digestion scheme with concentrated q-HNO_3 and concentrated HF (*Optima*), as described in Morton et al. (2013). All samples were analyzed using the E2 ICP-MS. The 2014 aerosol samples were analyzed for UHP-soluble and total trace element concentrations. The 2015 aerosol samples were analyzed for total trace element concentrations only. To determine the overall precision, selected aerosol samples were analyzed in triplicate and the average RSD values were calculated and applied to all other aerosol samples.

Ten-day (240-hour) air mass back trajectories (AMBTs) for the 2014 and 2015 field campaigns were simulated using the GDAS meteorology data set in the publicly available NOAA Air Resources Laboratory Hybrid Single-Particle Lagrangian Integrated Trajectory (HYSPLIT) model (Stein et al., 2015; Rolph, 2017). Even though samples were collected 2–3 m above sea level, arrival heights of 500, 1,000, and 1,500 m were chosen to represent trajectories within and above the marine boundary layer (400 to 1,200 m thickness).

Results

Figure 2 shows the wind speeds over the course of both field campaigns. For 2014, the average wind speed was 2.5 ± 0.8 m s^{-1} and for 2015, the average wind speed was

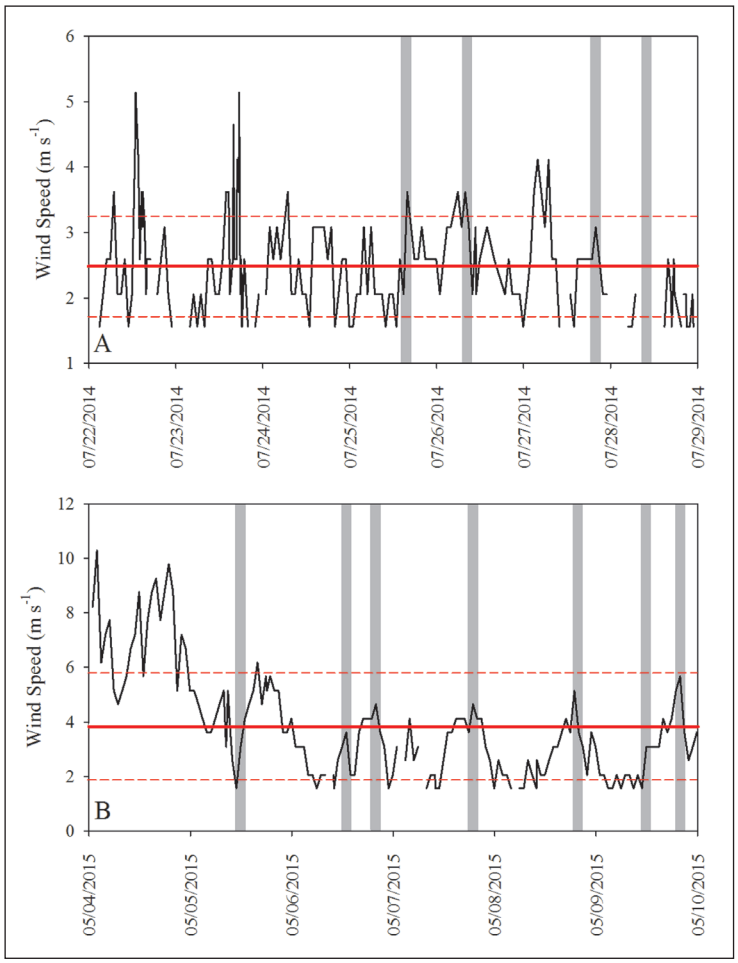

Figure 2: Ancillary data. Wind speeds over the course of the 2014 **(A)** and 2015 **(B)** field campaigns. The red solid line indicates the average wind speed and the red dashed lines indicating ±1 S.D. The grey bars represent when paired microlayer and water column samples were collected. DOI: https://doi.org/10.1525/elementa.237.f2

3.8 ± 2.0 m s^{-1}. The grey shaded bars indicate when sea surface microlayer and underlying water column sample pairs were collected. Overall, the sampling took place when wind speeds were less than 4 m s^{-1} in 2014 and less than 6 m s^{-1} in 2015. There were no recorded rain events during the 2014 sampling period and only one rain event occurred during the 2015 sampling period (May 5, 2015, 17:00–18:00 UTC) after the first microlayer and water column paired sampling (May 5, 2015, 12:00 UTC).

Tracking aerosols

An aerosol depth model (Naval Research Laboratory: http://www.nrlmry.navy.mil/aerosol/) was used to explore whether the air column over the sampling location contained high or low concentrations of dust. This model uses global meteorological fields from the Navy Operational Global Atmospheric Prediction System (NOGAPS; Hogan and Rosmond, 1991; Hogan and Brody, 1993) to forecast dust concentrations at 6-hour intervals. **Figures 3** and **4** show the model output during the 2014 and 2015 field campaigns, respectively. Each panel corresponds to a microlayer and water column collection time point associated with a 24-hour integrated aerosol sample. In 2014, there appears to have been dust over the study site during three of the four sampling time points (**Figure 3**) from July 26 to July 28. In 2015, there does not appear to have been dust over the study site during the five sampling time points (**Figure 4**).

"Dusty" season trace element distributions in the sea surface microlayer, underlying water column, and atmospheric aerosols

Trace element concentrations in the dissolved and total particulate fractions of the sea surface microlayer and underlying water column as well as the atmospheric aerosols for the 2014 field campaign are presented in **Figures 5, 6,** and **7**. Overall sample replicates showed ±20% variability with the exception of the dissolved Al, Fe, and Zn concentrations on July 26, 2014, (approximately ±50%). Given

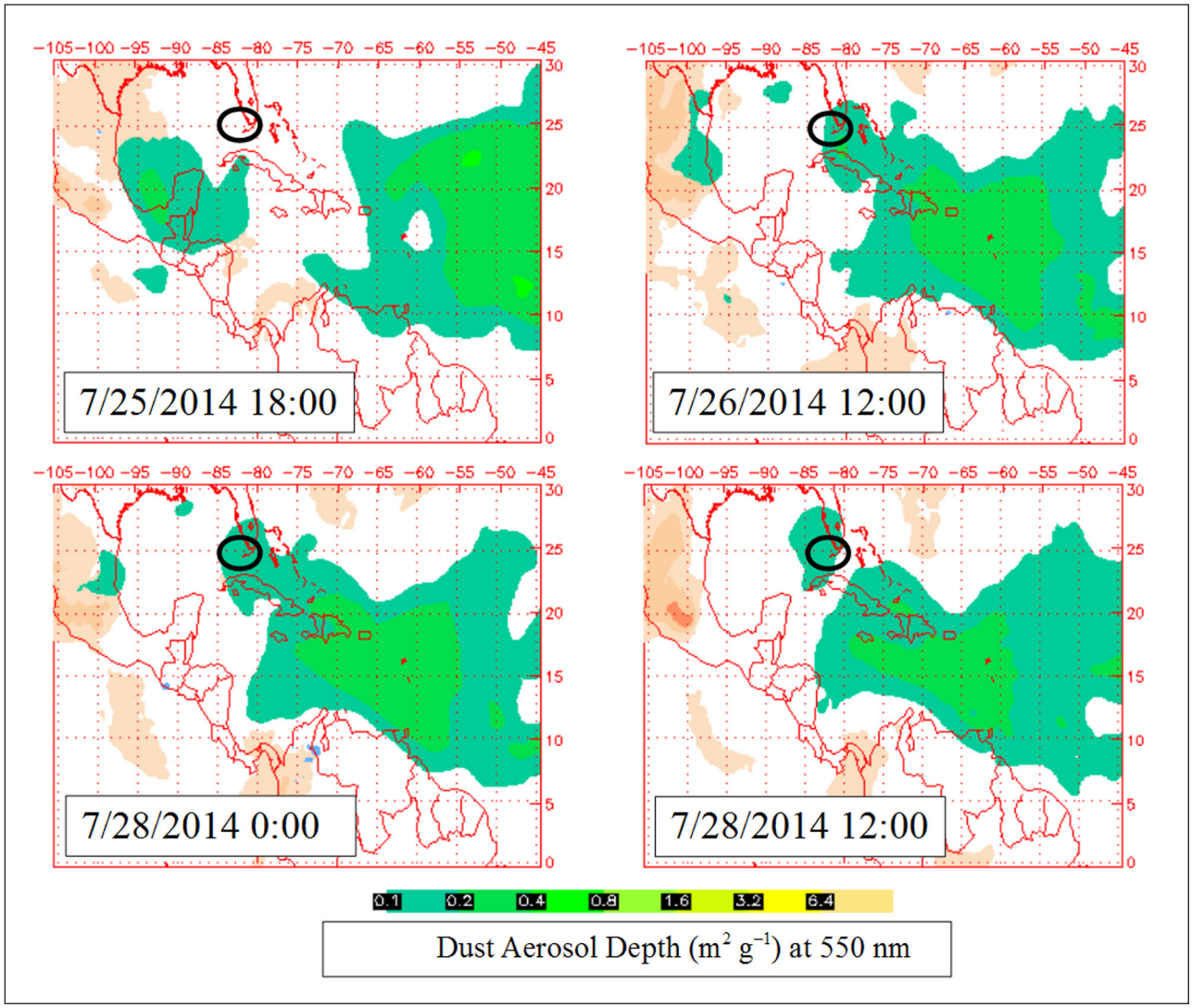

Figure 3: 2014 aerosol optical depths. Modeled aerosol optical depths (Naval Research Laboratory; http://www.nrlmry.navy.mil/aerosol/) for the 2014 sea surface microlayer and underlying water column sampling periods. The study site is circled in black and the green contour lines (following the color scale bar) represent the optical dust depth (based on light scattering at 550 nm). DOI: https://doi.org/10.1525/elementa.237.f3

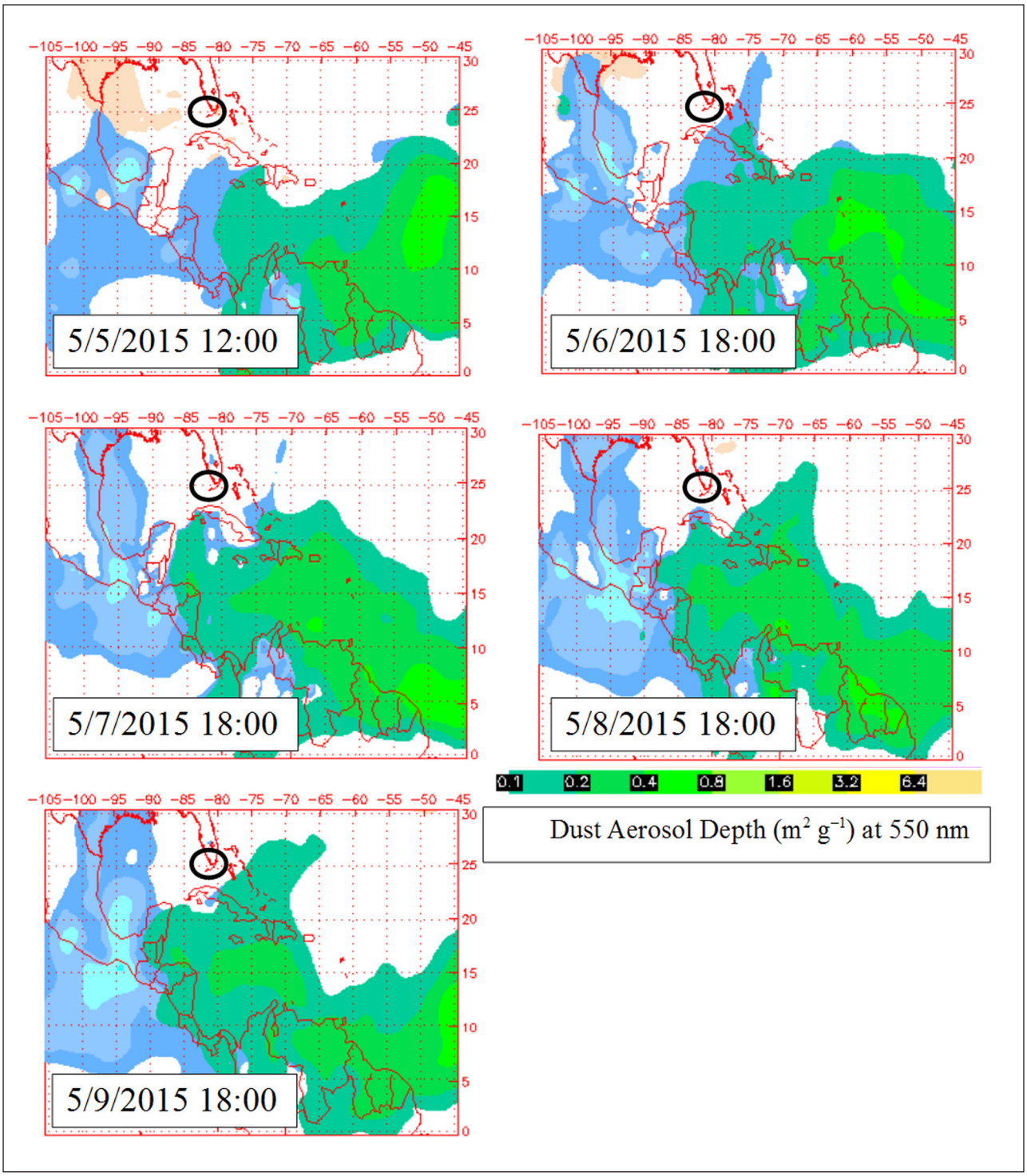

Figure 4: 2015 aerosol optical depths. Modeled aerosol optical depths (Naval Research Laboratory; http://www.nrlmry.navy.mil/aerosol/) for the 2015 sea surface microlayer and underlying water column sampling periods. The study site is circled in black and the green contour lines (following the color scale bar) represent the optical dust depth (based on light scattering at 550 nm). DOI: https://doi.org/10.1525/elementa.237.f4

the potential heterogeneity of the microlayer (Wurl and Obbard, 2004), this variability is not unexpected. In the dissolved fraction, there is an overall trend that the microlayer and water column did not differ over the course of the four sampling days with the exception of Zn, where concentrations were often below the detection limit and, therefore, could not be compared directly (**Figure 6D**). Temporally, dissolved Al and Fe appeared higher in concentration on July 26 compared to July 25 (**Figures 5A** and **5D**); however, the difference is not significant considering the replicate variability. Geographically, most dissolved trace element concentrations were similar between the FB location and the AO on July 28 (**Figures 5A, 5D, 6A** and **6D**), with a slight decrease in the Ni concentration in the AO (**Figure 7A**) and a slight increase in the Pb concentration in the AO (**Figure 7D**).

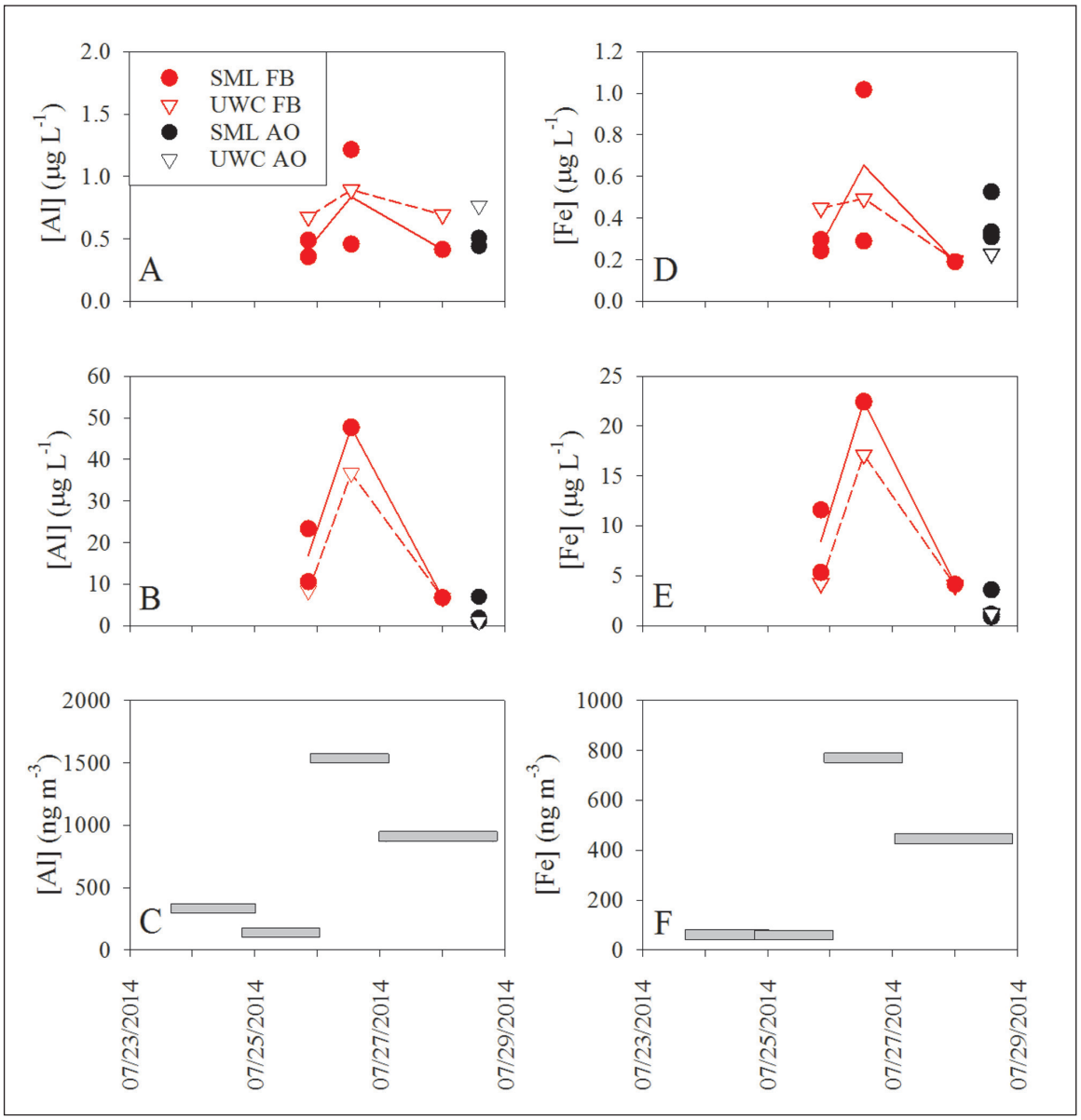

Figure 5: 2014 Al and Fe concentrations. Dissolved Al **(A)** and Fe **(D)** concentrations in the sea surface microlayer (SML) and underlying water column (UWC) in the Florida Bay (FB; solid red circles = SML; open red triangles = UWC) and coastal Atlantic Ocean (AO; solid black circles = SML; open black triangles = UWC). Total particulate Al **(B)** and Fe **(E)** concentrations in the SML and UWC in the FB and AO. Total Al **(C)** and Fe **(F)** concentrations in 24-hour integrated aerosol samples. Solid red lines show the average microlayer concentrations and the dashed red lines show the average water column concentrations. DOI: https://doi.org/10.1525/elementa.237.f5

As with the dissolved trace elements, in the particulate fraction the microlayer and water column did not differ over the four days, with the exceptions of Ni, where water column concentration on July 25 was higher compared to the microlayer (**Figure 7B**), and Zn, where water column concentrations were higher on July 25 and July 26 compared to the microlayer (**Figure 6E**). When examining temporal changes in the particulate trace element concentrations in the microlayer and water column samples, a pattern emerges. Most elements increased by factors of 2 to 5 on July 26, 2014, when compared to the previous day (**Figures 5B, 5E, 6B, 6E, 7B** and **7E**). A similar pattern emerges in the aerosol samples. For all trace elements, concentrations in the third 24-hour integrated sample (start date: July 26, 2014) were elevated 1.6 to 13 times compared to the concentrations in the previous sample (**Figures 5C, 5F, 6C, 6F, 7C** and **7F**).

"Non-dusty" season trace element distributions in the sea surface microlayer, underlying water column, and atmospheric aerosols

Dissolved and particulate trace element concentrations in the sea surface microlayer and underlying water column, as well as the atmospheric aerosols for the 2015 field campaign, are presented in **Figures 8, 9** and **10**. As with the 2014 samples, overall sample replicates showed ±20% variability with the few exceptions in the dissolved Zn concentrations on May 5 in SB and May 9 on LK (approximately ±40%; **Figure 9D**). In the dissolved fraction, there is an overall trend that the microlayer and water column

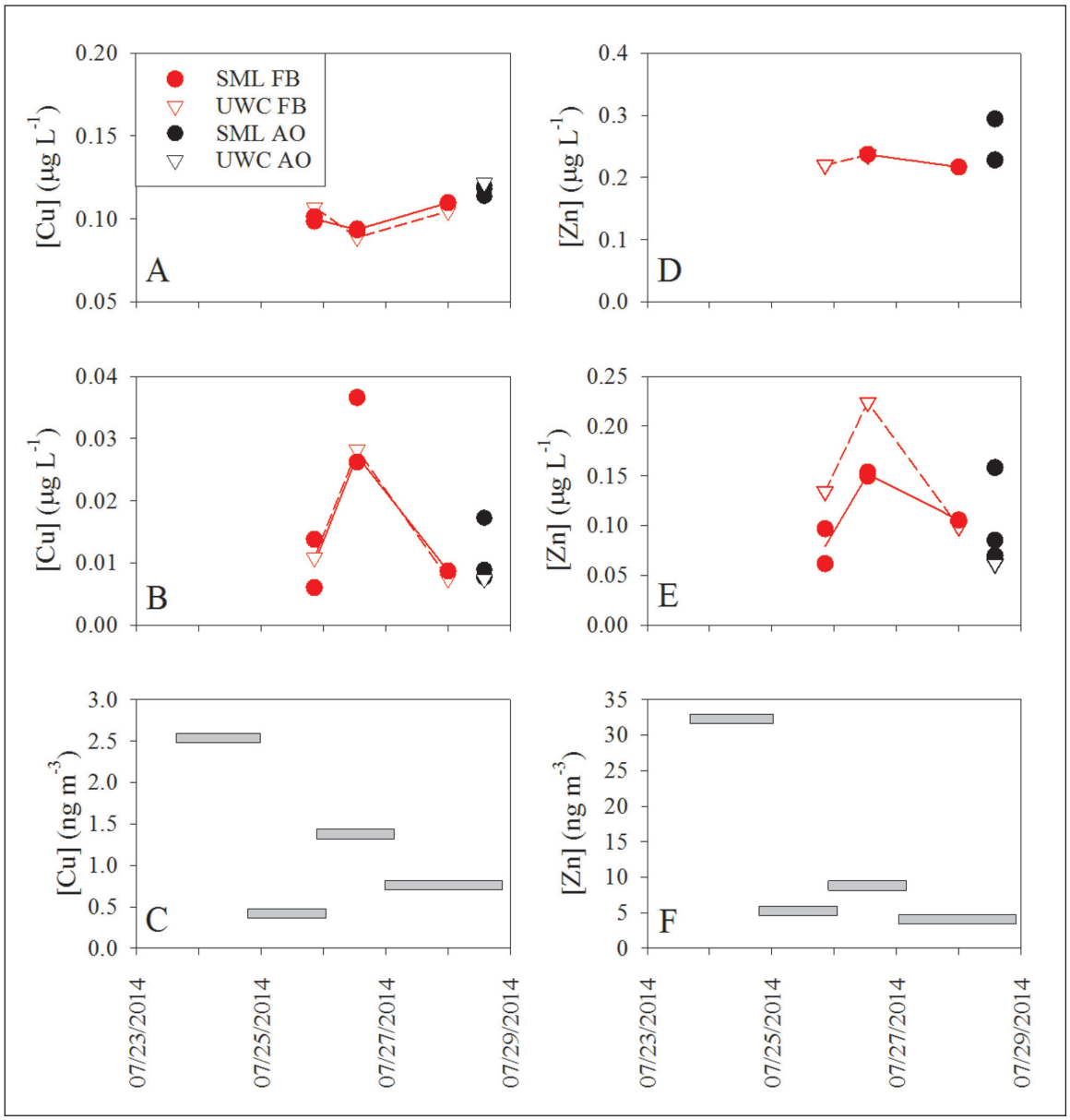

Figure 6: 2014 Cu and Zn concentrations. Dissolved Cu **(A)** and Zn **(D)** concentrations in the sea surface microlayer (SML) and underlying water column (UWC) in the Florida Bay (FB; solid red circles = SML; open red triangles = UWC) and coastal Atlantic Ocean (AO; solid black circles = SML; open black triangles = UWC). Total particulate Cu **(B)** and Zn **(E)** concentrations in the SML and UWC in the FB and AO. Total Cu **(C)** and Zn **(F)** concentrations in 24-hour integrated aerosol samples. Solid red lines show the average microlayer concentrations and the dashed red lines show the average water column concentrations. DOI: https://doi.org/10.1525/elementa.237.f6

did not differ over the course of the study with the exceptions of Al and Fe, where microlayer concentrations were consistently lower compared to the water column (**Figures 8A** and **8D**) and Zn, where microlayer concentrations were consistently higher compared to the water column (**Figure 9D**). There were some slight increases and decreases from day to day in the dissolved trace elements concentrations; however, the overall dissolved trace element distributions did not seem to vary over time except for Zn, where microlayer concentration increased 2.5 times between May 7 and 8 in SB (**Figure 9D**). The dissolved trace element concentrations did, however, vary between the two locations as the dissolved trace element concentrations at LK were significantly lower in comparison to the dissolved trace element concentrations at SB (**Figures 8A, 8D, 9A** and **10D**).

As with the dissolved trace elements, the microlayer and water column particulate fractions do not differ over the course of the study with the exceptions of Al and Fe, where water column concentrations were consistently higher than in the microlayer (**Figures 8B** and **8E**). Particulate Al, Fe, and Pb were significantly lower in concentration at LK compared to SB, illustrating the difference between the two sites (**Figures 8B, 8E** and **10E**). When examining the temporal change in the microlayer and water column samples, no clear pattern emerges. The atmospheric aerosols concentrations were fairly low throughout the campaign (**Figures 9C, 9F** and **10C**) with the exceptions of Al

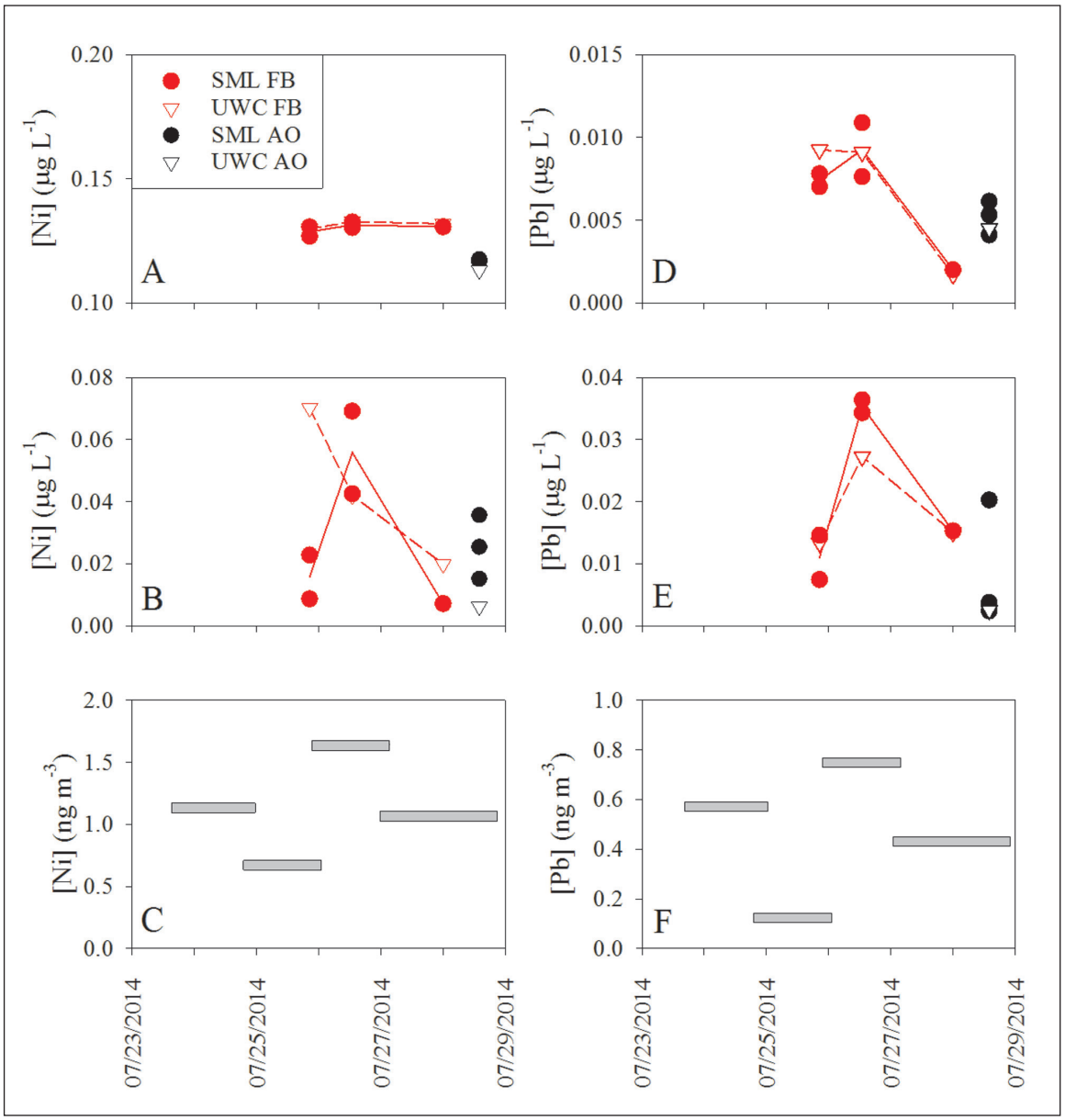

Figure 7: 2014 Ni and Pb concentrations. Dissolved Ni **(A)** and Pb **(D)** concentrations in the sea surface microlayer (SML) and underlying water column (UWC) in the Florida Bay (FB; solid red circles = SML; open red triangles = UWC) and coastal Atlantic Ocean (AO; solid black circles = SML; open black triangles = UWC). Total particulate Ni **(B)** and Pb **(E)** concentrations in the SML and UWC in the FB and AO. Total Ni **(C)** and Pb **(F)** concentrations in 24-hour integrated aerosol samples. Solid red lines show the average microlayer concentrations and the dashed red lines show the average water column concentrations. DOI: https://doi.org/10.1525/elementa.237.f7

(**Figure 8C**), Fe (**Figure 8F**), and Pb (**Figure 10F**), where concentrations increased by a factor of 2 to 8 on May 9, 2015.

Discussion

Dusty season vs. non-dusty season

Aerosols originate from many sources, including desert regions, biomass burning, and anthropogenic emissions. The regions where the aerosols were initially generated have often been correlated with their chemistry to speculate on their impacts to the surface ocean (Spokes and Jickells, 1996; Baker et al., 2006; Sedwick et al., 2007) and to inform predictive models concerning the marine carbon cycle (e.g. Tagliabue et al., 2014). There are several ways in which aerosol origin can be identified. In this study, the NOAA HYSPLIT AMBTs were used to identify aerosol origin. **Figure 11** shows example AMBTs for both the 2014 and 2015 field campaigns. The AMBT for July 26, 2014, shows a North African source (**Figure 11B**). Combining this model and the aerosol optical depth model, the aerosols collected for this day almost certainly originated from North Africa and presumably represent a typical summer Saharan dust event for the region (e.g. Prospero 1999; Trapp et al., 2010).

Other tracers of aerosol origin used in this study were elemental ratios, specifically Ti, V, Mn, and Fe normalized to Al. Aluminum is used as an indicator of lithogenic origin in aerosol composition and TE/Al ratios can reflect

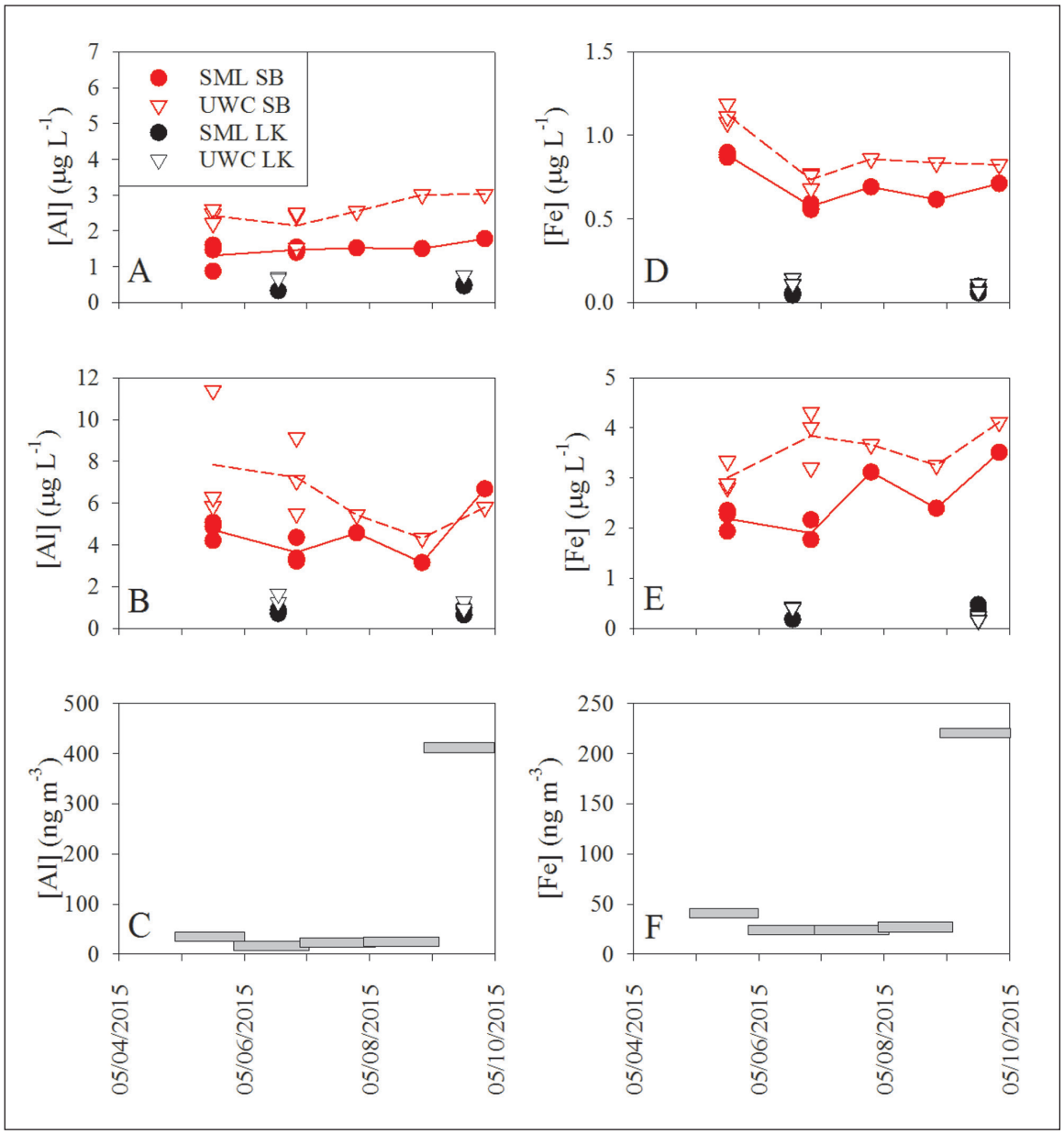

Figure 8: 2015 Al and Fe concentrations. Dissolved Al **(A)** and Fe **(D)** concentrations in the sea surface microlayer (SML) and underlying water column (UWC) in the Summerland Key Bay (SB; solid red circles = SML; open red triangles = UWC) and Looe Key National Marine Sanctuary (LK; solid black circles = SML; open black triangles = UWC). Total particulate Al **(B)** and Fe **(E)** concentrations in the SML and UWC in the SB and LK. Total Al **(C)** and Fe **(F)** concentrations in 24-hour integrated aerosol samples. Solid red lines show the average microlayer concentrations and the dashed red lines show the average water column concentrations. DOI: https://doi.org/10.1525/elementa.237.f8

different mineralogical composition (Guieu et al., 2002). **Table 1** shows the Ti/Al, V/Al, Mn/Al, and Fe/Al ratios of four aerosol samples collected during the 2014 field campaign. The TE/Al ratios can be used to trace lithogenic aerosols, but should be interpreted with caution, as North African aerosols tend to have, for example, higher Fe/Al ratios compared to the global average upper continental crust (Shelley et al., 2015; **Table 1**). Three out of the four aerosol samples in the 2014 field campaign show similar Ti/Al, Mn/Al, and Fe/Al ratios that are comparable to the North African aerosol ratios. These three samples also had AMBTs suggesting that the air masses came from North Africa, whereas the lower Ti/Al, Mn/Al, and Fe/Al ratios on July 23 correspond to an AMBT that showed a marine origin (**Figure 11A**).

The dissolved trace element concentrations in the microlayer and water column showed little variability over the 2014 sampling time frame (**Figures 5, 6** and **7**), even with a significant dust event in the area. The UHP-soluble aerosol leaches collected for this field campaign showed low solubilities for trace elements such as Al and Fe (0.35 and 0.23%, respectively). Combined with the relatively high background concentrations of dissolved Al and Fe compared to the open ocean, these low solubilities could explain why there appears to be little to no effect on the dissolved trace element concentrations in the microlayer

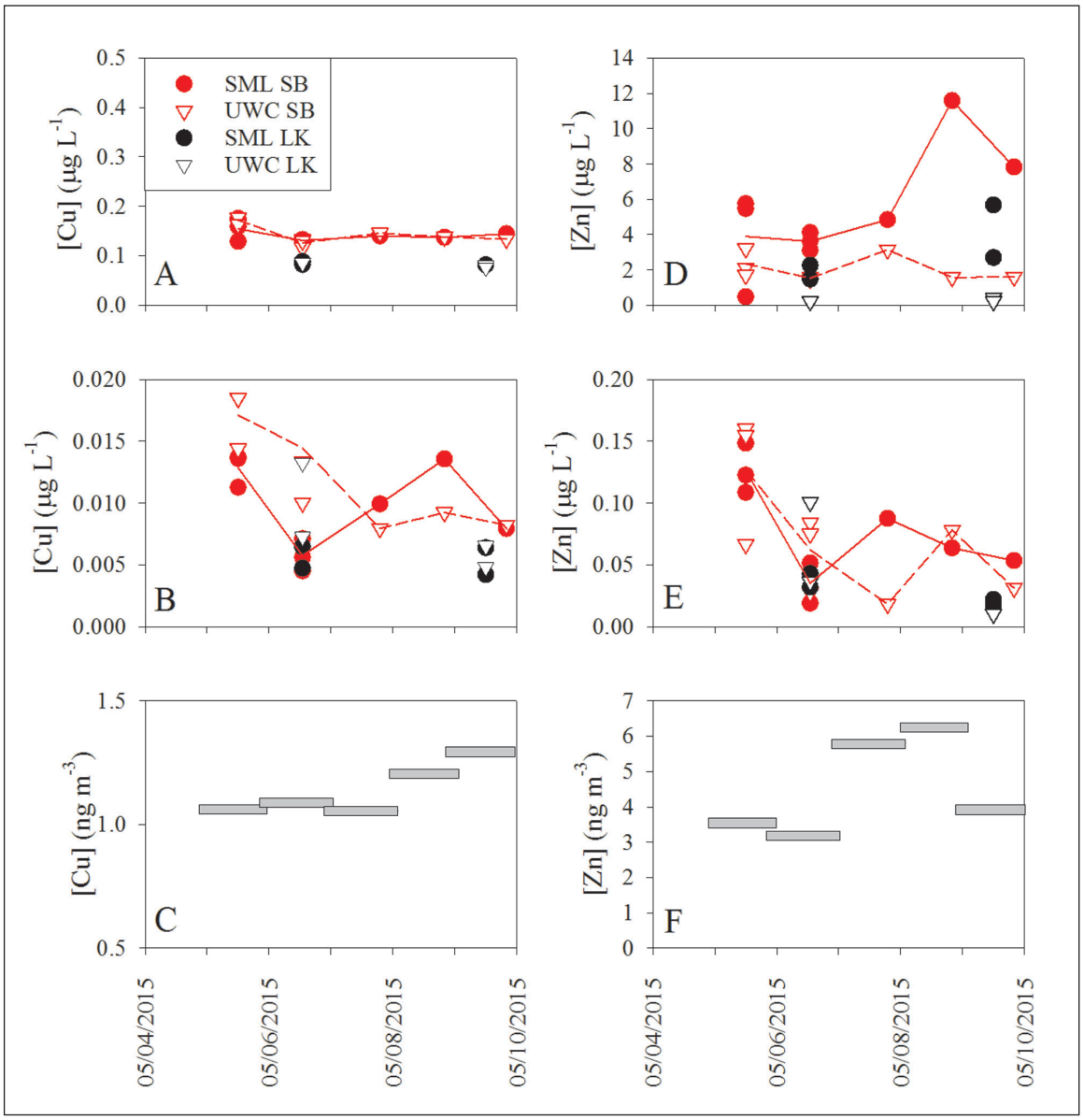

Figure 9: 2015 Cu and Zn concentrations. Dissolved Cu **(A)** and Zn **(D)** concentrations in the sea surface microlayer (SML) and underlying water column (UWC) in the Summerland Key Bay (SB; solid red circles = SML; open red triangles = UWC) and Looe Key National Marine Sanctuary (LK; solid black circles = SML; open black triangles = UWC). Total particulate Cu **(B)** and Zn **(E)** concentrations in the SML and UWC in the SB and LK. Total Cu **(C)** and Zn **(F)** concentrations in 24-hour integrated aerosol samples. Solid red lines show the average microlayer concentrations and the dashed red lines show the average water column concentrations. DOI: https://doi.org/10.1525/elementa.237.f9

from atmospheric deposition. When comparing the particulate trace element concentrations in the microlayer to the aerosol concentrations a different pattern emerges. As mentioned above, most trace element concentrations in the microlayer increased by factors of 2 to 5 on July 26, 2014, which coincides with an observed increase in atmospheric aerosol concentrations (**Figures 5, 6** and **7**). Hoffman et al. (1974) also observed high Fe concentrations off the coast of North Africa in the microlayer when there was significant continental dust.

Elemental ratios were also calculated for the microlayer and water column particulate samples collected during the 2014 field campaign to compare to the aerosol elemental ratios (**Table 2**). The microlayer ratios are very similar to the aerosol ratios, with three exceptions (all on July 28): the Ti/Al ratio in the AO (0.17 for the microlayer versus 0.06 for the aerosol) and the Mn/Al ratios in the FB (0.135 for the microlayer versus 0.009 for the aerosol) and the AO (0.024 for the microlayer versus 0.009 for the aerosol). The water column ratios are also very similar to the aerosol ratios, with five exceptions (all on July 28): the Ti/Al ratios on in the FB (0.23 for the water column versus 0.06 for the aerosol) and the AO (0.31 for the water column versus 0.06 for the aerosol), the V/Al ratio in the AO (0.23 for the water column versus 0.002 for the aerosol), the Mn/Al ratios in the FB (0.163 for the water column versus 0.009 for the aerosol) and the AO (0.070 for the water column versus 0.009 for the aerosol), and the

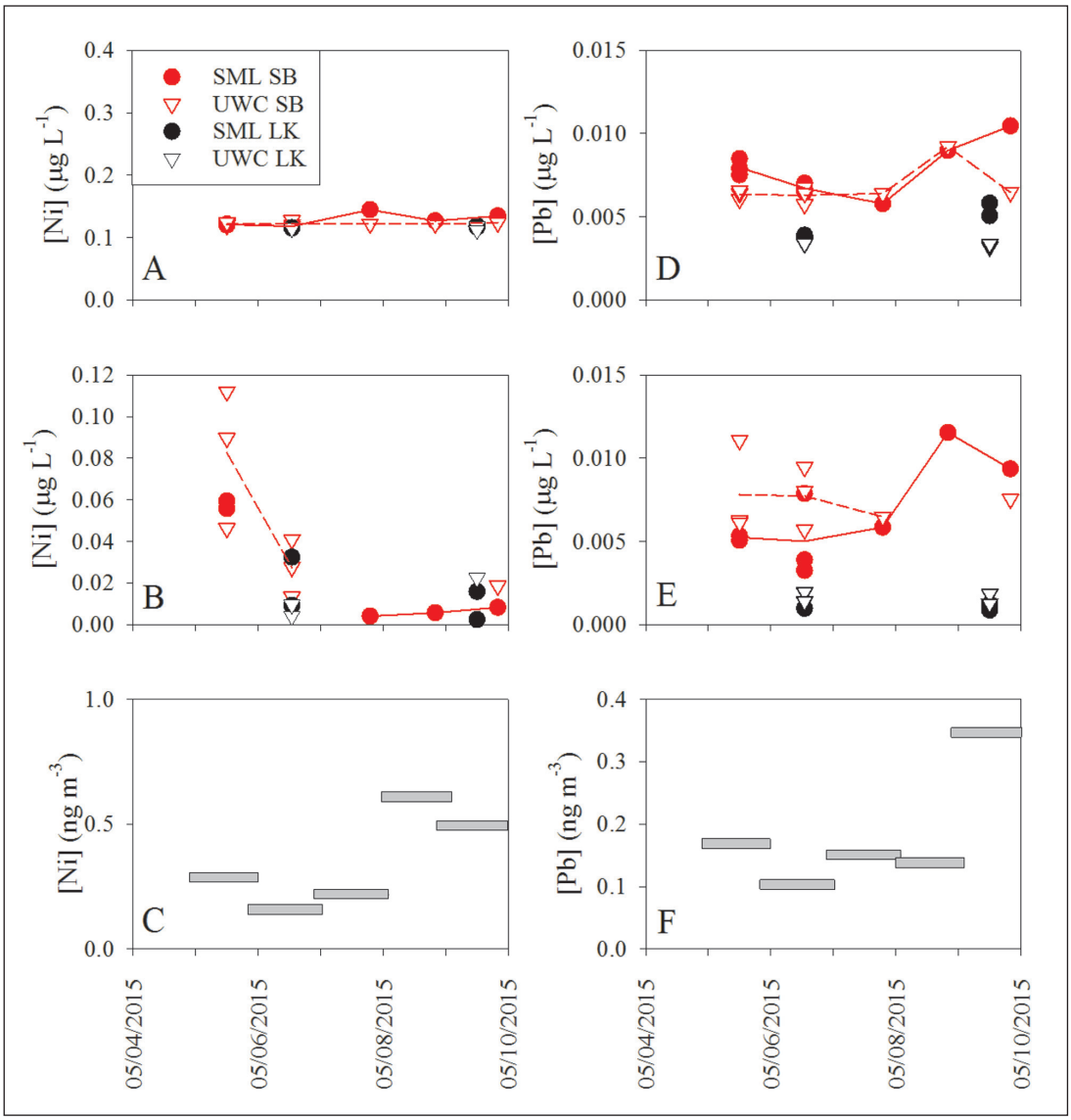

Figure 10: 2015 Ni and Pb concentrations. Dissolved Ni **(A)** and Pb **(D)** concentrations in the sea surface microlayer (SML) and underlying water column (UWC) in the Summerland Key Bay (SB; solid red circles = SML; open red triangles = UWC) and Looe Key National Marine Sanctuary (LK; solid black circles = SML; open black triangles = UWC). Total particulate Ni **(B)** and Pb **(E)** concentrations in the SML and UWC in the SB and LK. Total Ni **(C)** and Pb **(F)** concentrations in 24-hour integrated aerosol samples. Solid red lines show the average microlayer concentrations and the dashed red lines show the average water column concentrations. DOI: https://doi.org/10.1525/elementa.237.f10

Fe/Al ratio in the AO (1.07 for the water column versus 0.50 for the aerosol). The AO microlayer sample, in general, appears to be enriched in trace elements compared to the aerosol sample, indicative of possible scavenging onto particles. This observation further applies to the AO water column sample, where all four ratios are enriched compared to both the corresponding aerosol and microlayer samples. The FB ratios show some enrichment in the microlayer and water column samples compared to the aerosol samples, but not as strongly as in the AO sample.

The aerosols collected during the 2015 field campaign originated from either North America (**Figure 11C**) or the Atlantic Ocean (**Figure 11D**). Their relatively low trace element concentrations (**Figures 8, 9** and **10**) compared to the North African aerosols collected in 2014 support our conclusion that sampling in 2015 occurred during a low dust period which corresponds to a non-dust season.

The dissolved and total particulate trace element concentrations in the microlayer and water column showed little variability during the 2015 field campaign (**Figures 8, 9** and **10**). As we believe that dust deposition was low in the region, the concentrations were likely influenced by other factors. Rising bubbles from the underlying water column act as another source of trace elements to the microlayer (Hardy, 1982; Cuong et al., 2008) when there is no significant dust in the region. Cu, Zn, Ni, and Pb concentrations in the 2015 microlayer samples indicate a trace element composition similar to the corresponding water column, suggesting an underlying water column source (**Figures 9A, 9D, 10A** and **10D**). There was notable depletion in the dissolved Al and Fe

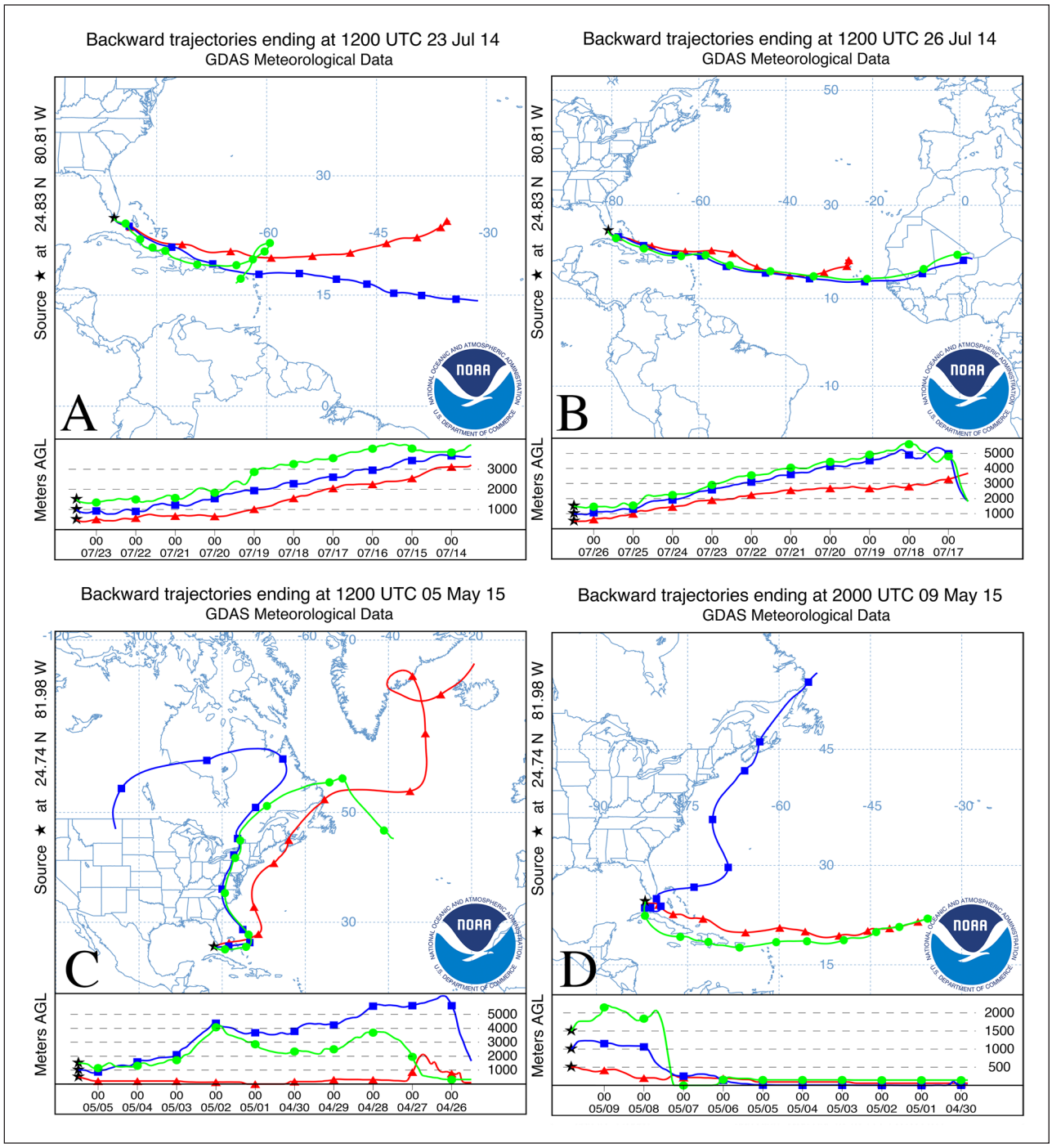

Figure 11: Air mass back trajectories. Ten-day air mass back trajectory (AMBT) simulations from example microlayer and water column sampling periods in 2014 (**A** and **B**) and 2015 (**C** and **D**), with arrival heights of 500 m (red), 1,000 m (blue), and 1,500 m (green). DOI: https://doi.org/10.1525/elementa.237.f11

concentrations in the microlayer compared to the water column (**Figures 8A** and **8D**). This phenomenon has been observed elsewhere: Ebling and Landing (2015) showed depletion in dissolved Al and Fe in the Bay of Villefranche, France, when there was no significant atmospheric input to the microlayer. Depletions in dissolved constituents in the microlayer that are statistically significant are difficult to maintain in the face of molecular diffusion from the underlying water column. Diffusive mixing with a molecular diffusion coefficient on the order of 10^{-5} cm^2 s^{-1} yields displacement of about 100 µm in less than 10 seconds. Thus, significant depletion that is long-lived (or perhaps at steady-state) would require a removal mechanism that is fast relative to diffusion. There was notable depletion in particulate Al and Fe in the microlayer compared to the water column as well. Hunter (1980) also reported depletion in particulate Fe and Mn in the North Sea. While Hunter's argument was that lithogenic trace elements such as Mn and Fe would not favor the organic rich microlayer, apparent depletions in particles in the microlayer could result from sediment resuspension in shallow environments (such as SB) where the underlying

Table 1: Comparison of selected trace element ratios[a] in aerosols of this study with aerosols of North African origin from other studies in the region, oceanic aerosols of North African origin, and the global average upper continental crust. DOI: https://doi.org/10.1525/elementa.237.t1

Location (date, 2014)	Ti/Al	V/Al	Mn/Al	Fe/Al	Reference
Florida Keys (July 23)[b]	0.01 (0.001)	0.001 (0.0001)	0.004 (0.0003)	0.20 (0.02)	This study
Florida Keys (July 24)	0.05 (0.005)	0.006 (0.0005)	0.010 (0.0008)	0.47 (0.04)	This study
Florida Keys (July 25)	0.06 (0.006)	0.002 (0.0002)	0.009 (0.0007)	0.50 (0.04)	This study
Florida Keys (July 26)	0.06 (0.006)	0.002 (0.0002)	0.009 (0.0007)	0.50 (0.04)	This study
Miami/Barbados	–[c]	–	0.012	0.70	Trapp et al., 2010
Barbados	–	0.002	0.011	0.51	Arimoto et al., 1995
At sea	0.08	0.003	0.013	0.77	Shelley et al., 2015
At sea	0.12	0.005	0.012	0.66	Buck et al., 2010
At sea	–	–	0.010	0.58	Baker et al., 2013
Global average upper continental crust	0.04	0.0007	0.007	0.44	Taylor and McLennan, 1995

[a]By mass, with 1 S.D. values for aerosols from this study given in parentheses.
[b]Aerosol sample not of North African origin.
[c]Not available.

Table 2: Selected trace element ratios (by mass) in particulate samples of the sea surface microlayer and underlying water column during the 2014 field campaign. DOI: https://doi.org/10.1525/elementa.237.t2

Sample type	Date	Location[a]	Ti/Al	V/Al	Mn/Al	Fe/Al
Sea surface microlayer	July 25	FB	0.08	0.003	0.012	0.50
	July 26	FB	0.06	0.002	0.013	0.47
	July 28	FB	0.09	0.003	0.135	0.61
	July 28	AO	0.17	0.005	0.024	0.57
Underlying water column	July 25	FB	0.09	0.003	0.016	0.51
	July 26	FB	0.08	0.002	0.016	0.47
	July 28	FB	0.23	0.003	0.163	0.60
	July 28	AO	0.31	0.023	0.070	1.07

[a]FB indicates Florida Bay; AO, coastal Atlantic Ocean.

water column becomes enriched in particles. In addition, particle settling will constantly remove particles from the microlayer into the water column.

Residence times of atmospheric trace elements in the sea surface microlayer

An important parameter when studying the impact of atmospheric deposition to the microlayer is the residence time (τ) of the variable of interest: the mean time of replacement based on the reservoir inventory and the input flux. In this study residence times for dissolved and particulate trace elements were calculated using the following equation:

$$\tau = [TE]_{SML} \times \delta / J_{aerosol} \quad (1)$$

where $[TE]_{SML}$ is the concentration of trace element (TE) in the sea surface microlayer (SML), δ is the microlayer thickness (50 μm; Ebling and Landing, 2015), and $J_{aerosol}$ is the flux of aerosol trace element which can be calculated from the aerosol concentration and the dry deposition velocity for mineral dust of approximately 1,000 m d^{-1} (Duce et al., 1991). Residence times were calculated for July 26, 2014, in FB and July 28, 2014, in both locations (FB and AO), as these were the days with significant dust in the region (**Figure 9**). Residence times for dissolved trace elements were calculated from the dissolved microlayer trace element concentrations and fluxes of UHP-soluble aerosol trace elements. Residence times for particulate trace elements were calculated from the total particulate trace element concentrations and the fluxes of total aerosol trace elements.

Table 3: Residence times (τ in minutes) of trace elements in sea surface microlayer samples from the 2014 field campaign. DOI: https://doi.org/10.1525/elementa.237.t3

Location, date, form	Al	Fe	Ni	Cu	Zn	Pb
FB, July 26, dissolved	12 (7)[a]	26 (20)	50 (5)	180 (7)	14 (3)	94 (25)
FB, July 28, dissolved	5.3 (1.9)	8.2 (4.1)	49 (5)	200 (8)	10 (2)	14 (3)
AO, July 28, dissolved	6.2 (0.6)	8.1 (1.7)	44 (5)	210 (10)	12 (2)	37 (7)
FB, July 26, particulate	2.2 (0.2)	2.1 (0.1)	2.5 (1.1)	1.7 (0.5)	1.3 (0.4)	3.4 (0.6)
FB, July 28, particulate	0.54 (0.04)	0.67 (0.04)	0.48 (0.22)	0.84 (0.25)	1.9 (0.5)	2.5 (0.5)
AO, July 28, particulate	0.27 (0.31)	0.30 (0.29)	1.7 (1.1)	1.1 (1.0)	1.8 (2.8)	1.5 (2.6)

[a]Parenthetic values are 1 S.D. of the residence time.

Table 3 shows the residence times for dissolved and particulate trace elements in the microlayer. Residence times of dissolved trace elements ranged from 5.3 minutes for Al to 210 minutes (3.5 hours) for Cu. Residence times of particulate trace elements ranged from 0.27 minutes (16 seconds) for Al to 3.4 minutes for Pb. Generally, residence times were longer in FB on July 26 compared to July 28. While the literature is consistent in the observation that particulate trace elements are usually enriched in the microlayer, it is less consistent with respect to the particle residence times in the microlayer, with reports ranging from a few seconds to tens of minutes (e.g., Duce et al., 1972; Hoffman et al., 1974; Hardy et al., 1985). Hoffman et al. (1974) estimated the residence time of particulate Fe in the microlayer as a few seconds for a Saharan dust deposition event, whereas Eisenreich (1982) estimated the microlayer residence times for a suite of total trace elements (dissolved plus particulate) in the microlayer of Lake Superior ranging from 20 to 79 minutes. In our 2014 FB experiment, the inventory of particulate Fe in the microlayer (50 μm thick) on July 26 was 1,150 ng m^{-2}. Using an aerosol dry deposition velocity of 1,000 m d^{-1} (~1 cm s^{-1}; typical for 1 μm mineral dust aerosols), the aerosol Fe concentration of 774 ng m^{-3} should result in the deposition of 537 ng m^{-2} min^{-1}. This calculation yields a residence time (τ) for particulate Fe in the microlayer (with respect to aerosol Fe input) on the order of 2 minutes (**Table 3**). When the aerosol Fe concentration dropped to 448 ng m^{-3}, the deposition rate should have dropped to 311 ng m^{-2} min^{-1}. If the decrease in the particulate Fe concentration in the microlayer between July 26 and July 28 was in response to the lower aerosol concentration, then the loss rate of particulate Fe from the microlayer must have been greater than the input rate of 311 ng m^{-2} min^{-1}, yielding τ = ~ 1 minute with respect to particulate Fe loss. The fact that the dissolved and particulate Fe concentrations in the underlying water column closely track those in the microlayer supports our conclusion that there must be rapid transfer of particles through the microlayer and into the upper ocean. These short residence time estimates for particulate Fe in the microlayer are not inconsistent with an upper limit estimate for the Stokes settling velocity of a 1 μm particle (ρ = 2.5) in pure seawater on the order of 50 μm min^{-1}. However, it is unlikely that such rapid settling velocities would apply for particles that are interacting with the gel-like, organic-rich film that characterizes the microlayer (Wurl and Holmes, 2008).

While the residence times for dissolved and particulate trace elements in this study are reasonably consistent with those determined from these previous studies, as well as from controlled tank experiments (Hardy et al., 1985; Ebling et al., unpublished data), the absolute values must be taken with caution. The aerosol deposition velocity of 1,000 m d^{-1} is probably a lower limit because it accounts for aerosol dry deposition only. Including wet deposition, which often accounts for about 50% of the total aerosol deposition, raises the bulk deposition velocity to about 2,000 m d^{-1} (Kadko et al., 2015). Using this higher bulk deposition velocity would lower the residence times by a factor of two. Furthermore, the aerosol sample from July 26, 2014, represents a 24-hour integrated sample, when the actual aerosol concentrations during that period may have varied considerably. Given the apparently very short residence times for both dissolved and particulate trace elements in the microlayer, short-term variations in the actual aerosol concentrations would produce proportional short-term variations in the fluxes and inverse effects on the residence times (Eq. 1). External factors such as wind (**Figure 2**) and waves also vary on short times scales compared to the 24-hour integrated aerosol sampling, which can also complicate residence time calculations as the microlayer is greatly affected by these factors (Cunliffe et al., 2013).

Conclusions

In summary, this study investigated dissolved and particulate trace element concentrations in the sea surface microlayer, underlying water column, and atmospheric aerosols during "dusty" (July 2014) and "non-dusty" (May 2015) periods in the Florida Keys. We observed a significant North African dust event during the 2014 field campaign. In turn, we observed elevated total particulate trace element concentrations in the microlayer during this event. From this dust event, residence times of dissolved and particulate trace elements in the microlayer ranged from a few minutes to a few hours. While the pro-

cesses that could alter the trace element concentrations and dissolved/particulate fractionations within the microlayer were not explored in this study, the residence times suggest that trace elements are retained long enough in the microlayer to be altered chemically and biologically. The next step will be to look at the organic complexation of trace elements as well as the biological response of various microorganisms found in the microlayer during atmospheric deposition events. Both processes will be explored from samples collected in the Florida Keys during the summer months of 2016.

Data Accessibility Statement

Seawater trace element concentrations: Biological & Chemical Oceanography Data Management Office (BCO-DMO).

Aerosol trace element concentrations: BCO-DMO.

Acknowledgements

The authors would like to thank Jason Westrich and Erin Lipp for their invaluable help with experimental design and sample collection. Thanks go to the Keys Marine Laboratory and the MOTE Tropical Research Laboratory for the use of their facilities. The authors would also like to thank two anonymous reviewers for their helpful feedback. A portion of this work was performed at the National High Magnetic Field Laboratory, which is supported by the NSF Cooperative Agreement DMR-1157490 and the State of Florida.

Funding information

NSF OCE-1357140 (to WML).

Competing interests

The authors have no competing interests to declare.

Author contributions

- Contributed to conception and design: AME, WML
- Contributed to acquisition of samples and data: AME
- Contributed to analysis and interpretation of data: AME, WML
- Drafted and/or revised the article: AME, WML
- Approved the submitted version for publication: AME, WML

References

Arimoto, R, Duce, RA, Ray, BJ, Eliis, WG, Jr., Cullen, JD and **Merrill, JT** 1995 Trace elements in the atmosphere over the North Atlantic. *J Geophys Res* **100**: 1199–213. DOI: https://doi.org/10.1029/94JD02618

Baker, AR, Adams, C, Bell, TG, Jickells, TD and **Ganzeveld, L** 2013 Estimation of atmospheric nutrient input to the Atlantic Ocean from 50°N to 50°S based on large-scale field sampling: iron and other dust-associated elements. *Global Biogeochem Cy* **27**: 755–67. DOI: https://doi.org/10.1002/gbc.20062

Baker, AR and **Croot, PL** 2010 Atmospheric and marine controls on aerosol iron solubility in seawater. *Mar Chem* **120**: 4–13. DOI: https://doi.org/10.1016/j.marchem.2008.09.003

Baker, AR, Jickells, TD, Witt, M and **Linge, KL** 2006 Trends in the solubility of iron, aluminum, manganese, and phosphorus in aerosols collected over the Atlantic Ocean. *Mar Chem* **98**: 43–58. DOI: https://doi.org/10.1016/j.marchem.2005.06.004

Baker, AR, Landing, WM, Bucciarelli, E, Cheize, M, Fietz, S, Hayes, CT, et al. 2016 Trace element and isotope deposition across the air-sea interface: progress and research needs. *Phil Trans R Soc A*. DOI: https://doi.org/10.1098/rsta.2016.0190

Barker, DR and **Zeitlin, H** 1972 Metal-ion concentrations in sea-surface microlayer and size-separated atmospheric aerosol samples in Hawaii. *J Geophy Res* **77**: 5076–86. DOI: https://doi.org/10.1029/JC077i027p05076

Berger, CJM, Lippiatt, SM, Lawrence, MG and **Bruland, KW** 2008 Application of a chemical leach technique for estimating labile particulate aluminum, iron, and manganese in the Columbia River plume and coastal waters off Oregon and Washington. *J Geohys Res,* **113**. DOI: https://doi.org/10.1029/2007JC004703

Boyd, PW, Mackie, DS and **Hunter, KA** 2010 Aerosol iron deposition to the surface ocean – modes of iron supply and biological response. *Mar Chem* **120**: 128–43. DOI: https://doi.org/10.1016/j.marchem.2009.01.008

Brügmann, L, Bernard, PC and **van Grieken, R** 1992 Geochemistry of suspended matter from the Baltic Sea. *Mar Chem* **38**: 303–23. DOI: https://doi.org/10.1016/0304-4203(92)90039-D

Buck, CS, Landing, WM, Resing, JA and **Measures, CI** 2010 The solubility and deposition of aerosol Fe and other trace elements in the North Atlantic Ocean: observations from the A16N CLIVAR/CO2 repeat hydrography section. *Mar Chem* **120**: 57–70. DOI: https://doi.org/10.1016/j.marchem.2008.08.003

Cunliffe, M, Engel, A, Frka, S, Gašparović, B, Guitart, C, Murrell, JC, et al. 2013 Sea surface microlayers: a unified physicochemical and biological perspective of the air-ocean interface. *Prog Oceanogr* **109**: 104–16. DOI: https://doi.org/10.1016/j.pocean.2012.08.004

Cunliffe, M, Salter, M, Mann, PJ, Whiteley, AS, Upstill-Goddard, RC and **Murrell, JC** 2009 Dissolved organic carbon and bacterial populations in the gelatinous surface microlayer of a Norwegian fjord mesocosm. *FEMS Microbiol Lett* **299**: 248–54. DOI: https://doi.org/10.1111/j.1574-6968.2009.01751.x

Cuong, DT, Karuppiah, S and **Obbard, JP** 2008 Distribution of heavy metals in the dissolved and suspended phase of the sea-surface microlayer, seawater column and in sediments of Singapore's coastal enrvironment. *Environ Monit Assess* **138**: 255–72. DOI: https://doi.org/10.1007/s10661-007-9795-y

Duce, RA, Quinn, JG, Olney, CE, Piotrowicz, SR, Ray, BJ and **Wade, TL** 1972 Enrichment of heavy

metals and organic compounds in the surface microlayer of Narragansett Bay, Rhode Island. *Science* **176**: 161–3. DOI: https://doi.org/10.1126/science.176.4031.161

Duce, RA and **Tindale, NW** 1991 Atmospheric transport if iron and its deposition in the ocean. *Limnol Oceanogr* **36**: 1715–26. DOI: https://doi.org/10.4319/lo.1991.36.8.1715

Dupont, CL, Buck, KN, Palenik, B and **Barbeau, K** 2010 Nickel utilization in phytoplankton assemblages from contrasting oceanic regimes. *Deep-Sea Res* **57**: 553–566. DOI: https://doi.org/10.1016/j.dsr.2009.12.014

Ebling, AM and **Landing, WM** 2015 Sampling and analysis of the sea surface microlayer for dissolve and particulate trace elements. *Mar Chem* **177**: 134–42. DOI: https://doi.org/10.1016/j.marchem.2015.03.012

Eisenreich, SJ 1982 Atmospheric role in trace metal exchange at the air-water interface. *J Great Lakes Res* **8**: 243–56. DOI: https://doi.org/10.1016/S0380-1330(82)71961-6

Franklin, MP, McDonald, IR, Bourne, DG, Owens, NJP, Upstill-Goddard, RC and **Murrell, JC** 2005 Bacterial diversity in the bacterioneuston (sea surface microlayer): The bacterioneuston through the looking glass. *Environ Microbiol* **7**: 723–36. DOI: https://doi.org/10.1111/j.1462-2920.2004.00736.x

Gledhill, M and **Buck, KN** 2012 The organic complexation of iron in the marine environment: a review. *Front Microbio* **3**: 1–17. DOI: https://doi.org/10.3389/fmicb.2012.00069

Grotti, M, Soggia, F, Abelmoschi, ML, Rivaro, P, Magi, E and **Frache, R** 2001 Temportal distribution of trace metals in Antarctic coastal waters. *Mar Chem* **76**: 189–209. DOI: https://doi.org/10.1016/S0304-4203(01)00063-9

Guieu, C, Loye-Pilot, MD, Ridame, C and **Thomas, C** 2002 Chemical characterization of the Saharan dust end-member: some biogeochemical implications for the western Mediterranean Sea. *J Geophy Res* **107**. DOI: https://doi.org/10.1029/2001JD000582

Hardy, JT 1982 The sea surface microlayer: biology, chemistry, and anthropogenic enrichment. *Prog Oceanogr* **11**: 307–28. DOI: https://doi.org/10.1016/0079-6611(82)90001-5

Hardy, JT, Apts, CW, Crecelius, EA and **Fellingham, GW** 1985 The sea-surface microlayer: fate and residence times of atmospheric metals. *Limnol Oceanogr* **30**: 93–101. DOI: https://doi.org/10.4319/lo.1985.30.1.0093

Hoffman, GL, Duce, RA, Walsh, PR, Hoffman, EJ and **Ray, BJ** 1974 Residence times of some particulate trace metals in the oceanic surface microlayer: significance of atmospheric deposition. *J Recher Atmos* **8**: 745–59.

Hogan, TF and **Brody, LR** 1993 Sensitivity studies of the Navy's global forecast model parameterizations and evaluations of improvements to NOGAPS. *Mon Wea Rev* **121**: 2372–95. DOI: https://doi.org/10.1175/1520-0493(1993)121<2373:SSOTNG>2.0.CO;2

Hogan, TF and **Rosmond, TE** 1991 The description of the navy operational global atmospheric prediction systems spectral forecast model. *Mon Weather Rev* **119**: 1786–1815. DOI: https://doi.org/10.1175/1520-0493(1991)119<1786:TDOTNO>2.0.CO;2

Hunter, KA 1980 Processes affecting particulate trace metals in the sea surface microlayer. *Mar Chem* **9**: 49–70. DOI: https://doi.org/10.1016/0304-4203(80)90006-7

Johnson, KS, Boyle, E, Bruland, K, Coale, K, Measures, C, Moffett, J, et al. 2007 Developing standards for dissolved iron in seawater. *Eos* **88**: 131–2. DOI: https://doi.org/10.1029/2007EO110003

Kadko, D, Landing, WM and **Shelley, RU** 2015 A novel tracer technique to quantify the atmospheric flux of trace elements to remote ocean regions. *J Geophys Res* **120**: 848–58. DOI: https://doi.org/10.1002/2014JC010314

Liss, P and **Duce, RA** 2005 *The sea surface and global change*. Cambridge University Press, UK.

Liu, X and **Millero, FJ** 2002 The solubility of iron in seawater. *Mar Chem* **77**: 43–54. DOI: https://doi.org/10.1016/S0304-4203(01)00074-3

Mackey, KRM, Chien, CT, Post, AF, Saito, MA and **Paytan, A** 2015 Rapid and gradual modes of aerosol trace metal dissolution in seawater. *Front MicroBio* **5**: 1–11. DOI: https://doi.org/10.3389/fmicb.2014.00794

Martin, JH and **Gordon, RM** 1988 Northeast Pacific iron distributions in relation to phytoplankton productivity. *Deep-Sea Res* **35**: 177–96. DOI: https://doi.org/10.1016/0198-0149(88)90035-0

Milne, A, Landing, W, Bizimis, M and **Morton, P** 2010 Determination of Mn, Fe, Co, Ni, Cu, Zn, Cd, and Pb in seawater using high resolution magnetic sector inductively coupled mass spectrometry (HR-ICP-MS). *Anal Chim Acta* **665**: 200–7. DOI: https://doi.org/10.1016/j.aca.2010.03.027

Morel, FMM and **Price, NM** 2003 The biogeochemical cycles of trace metals in the oceans. *Science* **300**: 944–7. DOI: https://doi.org/10.1126/science.1083545

Morton, PL, Landing, WM, Hsu, SC, Milne, A, Aguilar-Islas, AM, Baker, AR, et al. 2013 Methods for the sampling and analysis of marine aerosols: results from the 2008 GEOTRACES aerosol intercalibration experiment. *Limnol Oceanogr: Methods* **11**: 62–78. DOI: https://doi.org/10.4319/lom.2013.11.62

Prospero, JM 1999 Long-range transport of mineral dust in the global atmosphere: impact of African dust on the environment of the southeastern United States. *PNAS* **96**: 3396–3403. DOI: https://doi.org/10.1073/pnas.96.7.3396

Prospero, JM and **Mayol-Bracero, OL** 2013 Understanding the transport and impact of African dust on the

Caribbean Basin. *BAMS* **94**: 1329–37. DOI: https://doi.org/10.1175/BAMS-D-12-00142.1

Rolph, GD 2017 Real-time Environmental Applications and Display sYstem (READY). *NOAA Air Resources Laboratory*. http://ready.arl.noaa.gov/.

Sedwick, PN, Sholkovitz, ER and **Church, TM** 2007 Impact of anthropogenic combustion emissions on the fractional solubility of aerosol iron: evidence from the Sargasso Sea. *Geophy Geosys* **8**. DOI: https://doi.org/10.1029/2007GC001586

Shelley, RU, Morton, PL and **Landing, WM** 2015 Elemental ratios and enrichment factors in aerosols from the US-GEOTRACES North Atlantic transects. *Deep-Sea Res II* **116**: 262–72. DOI: https://doi.org/10.1016/j.dsr2.2014.12.005

Spokes, LJ and **Jickells, TD** 1996 Factors controlling the solubility of aerosol trace metals in the atmosphere and on mixing into seawater. *Aq Geochem* **1**: 355–74. DOI: https://doi.org/10.1007/BF00702739

Stein, AF, Draxler, RR, Rolph, GD, Stunder, BJB, Cohen, MD and **Ngan, F** 2015 NOAA's HYSPLIT atmospheric transport and dispersion modeling system. *Bull Amer Meteor Soc* **96**: 2059–77. DOI: https://doi.org/10.1175/BAMS-D-14-00110.1

Tagliabue, A, Aumont, O and **Bopp, L** 2014 The impact of different external sources of iron on the global carbon cycle. *Geophys Res Letters* **41**: 920–6. DOI: https://doi.org/10.1002/2013GL059059

Taylor, SR and **McLennan, SM** 1995 The geochemical evolution of continental crust. *Rev Geophys* **33**: 241–65. DOI: https://doi.org/10.1029/95RG00262

Trapp, JM, Millero, FJ and **Prospero, JM** 2010 Temporal variability of the elemental composition of African dust measured in trade wind aerosols at Barbados and Miami. *Mar Chem* **120**: 71–82. DOI: https://doi.org/10.1016/j.marchem.2008.10.004

Wurl, O and **Holmes, M** 2008 The gelatinous nature of the sea-surface microlayer. *Mar Chem* **110**: 89–97. DOI: https://doi.org/10.1016/j.marchem.2008.02.009

Wurl, O and **Obbard, JP** 2004 A review of pollutants in the sea-surface microlayer (SML): a unique habitat for marine organisms. *Mar Poll Bullet* **48**: 1016–30. DOI: https://doi.org/10.1016/j.marpolbul.2004.03.016

How to cite this article: Ebling, AM and Landing, WM 2017 Trace elements in the sea surface microlayer: rapid responses to changes in aerosol deposition. *Elem Sci Anth,* 5: 42, DOI: https://doi.org/10.1525/elementa.237

Domain Editor-in-Chief: Jody W. Deming, University of Washington, US

Knowledge Domain: Ocean Science

Part of an *Elementa* Special Feature: Sea-Surface Microlayer – Linking the Ocean and Atmosphere

Submitted: 14 March 2017 **Accepted:** 03 July 2017 **Published:** 01 August 2017

ELEMENTA Science of the Anthropocene

Elem Sci Anth is a peer-reviewed open access journal published by University of California Press.

OPEN ACCESS